Attitude Control of a Flexible Solar Power Satellite Using Self-tuning Iterative Learning Control

GAO Yuan, *WU Shunan*, *LI Qingjun**

School of Aeronautics and Astronautics, Sun Yat-sen University, Shenzhen 518107, P. R. China

(Received 20 June 2022; revised 11 August 2022; accepted 18 August 2022)

Abstract: This paper proposes a self-tuning iterative learning control method for the attitude control of a flexible solar power satellite, which is simplified as an Euler-Bernoulli beam moving in space. An orbit-attitude-structure coupled dynamic model is established using absolute nodal coordinate formulation, and the attitude control is performed using two control moment gyros. In order to improve control accuracy of the classic proportional-derivative control method, a switched iterative learning control method is presented using the control moments of the previous periods as feedforward control moments. Although the iterative learning control is a model-free method, the parameters of the controller must be selected manually. This would be undesirable for complicated systems with multiple control parameters. Thus, a self-tuning method is proposed using fuzzy logic. The control frequency of the controller is adjusted according to the averaged control error in one control period. Simulation results show that the proposed controller increases the control accuracy greatly and reduces the influence of measurement noise. Moreover, the control frequency is automatically adjusted to a suitable value.

Key words: iterative learning control; attitude control; solar power satellite; fuzzy control

CLC number: V448.22 **Document code:** A **Article ID:** 1005-1120(2022)04-0389-11

0 Introduction

Constructing solar power satellites in space and transmitting the energy to the ground is a potential way to generate clean and renewable energy and realize carbon neutrality in the future[1-2]. One difficulty of the solar power satellite is the precise attitude control of the ultra-large space structures because the attitude control accuracy would be influenced greatly by the ultra-flexibility of the structure or measurement noise[3].

Various researchers have studied the attitude control challenges of the ultra-large space structures, such as flexible solar sails[4-5] and flexible space manipulators[6]. However, the studies on attitude control of solar power satellites are not sufficient. Wie and Roithmayr proposed an orbit-attitude coupled control scheme for a solar power satellite using electric thrusters[7]. They found that the gravity gradient torque is the main attitude disturbance for ultra-large solar power satellite due to large moment of inertia. Wu et al.[8] proposed a robust optimal control algorithm with a disturbance rejection technique using internal model principle. However, Refs.[7-8] mainly concentrated on attitude control of a single rigid body. Zhang et al.[9] considered the flexibility of the transmitting antenna, solar arrays and truss structures, and presented a hybrid high/low bandwidth robust controller to alleviate the control-structure interaction problem. The attitude controllers in Refs.[8-9] were based on the accurate dynamic model of the flexible solar power satellite. However, the accurate dynamic model of such ultra-large spacecraft are not easy to established because of the uncertainties of numerous system parameters, clearances of connecters between structural modules,

*Corresponding author, E-mail address: liqingjun@sysu.edu.cn.

How to cite this article: GAO Yuan, WU Shunan, LI Qingjun. Attitude control of a flexible solar power satellite using self-tuning iterative learning control[J]. Transactions of Nanjing University of Aeronautics and Astronautics, 2022, 39(4): 389-399.

http://dx.doi.org/10.16356/j.1005-1120.2022.04.002

and complicated space perturbations for multiple flexible components. Thus, model-free attitude controllers are appealing for complicated ultra-large space structures.

The attitude control moments of the solar power satellite are usually periodic due to the periodic orbit and attitude[7]. In this case, the iterative learning control (ILC) method is very suitable to improve the control accuracy of current period by studying the control moments from previous periods and using them as feedforward control moments. ILC was firstly proposed in 1984 to improve the control accuracy of the robots performing repetitive operations[10]. One of the most important advantage of ILC is that it is a model-free control method that can be applied to complicated systems with uncertainties and large amplitude periodic disturbance[11]. In the recent years, ILC has been applied to the control systems in all kinds of engineering[12-13]. Particularly, ILC shows great potential to obtain high-precision attitude tracking control of satellites[14]. A high-order ILC controller is proposed to obtain precise Sun-facing and Earth-facing attitude control of a multi-rigid-body system of Multi-Rotary Joint Solar Power Satellite[15]. A smooth switch was adopted to avoid the sudden change of control moments, and a filter was used to reduce the influences of measurement noise and non-periodic signals. This method was further applied to a rigid-flexible coupled multi-body system of Multi-Rotary Joint Solar Power Satellite[16]. However, the parameters of the controller in Refs.[15-16] must be selected manually based on experiences. The concept of fuzzy logic was introduced to the design of ILC to reduce the number of tuning parameters and improve the convergence and stability of the controller in Refs.[17-18].

Thus, this paper aims to propose a self-tuning fuzzy ILC to maintain the Sun-facing attitude of a flexible solar power satellite. The rest of this paper is organized as follows. An orbit-attitude-structure coupled dynamic model of the flexible solar power satellite is built in Section 1. The implementation of the proportional-derivative (PD) controller, fuzzy PD controller, and fuzzy ILC controller are presented in Section 2. Section 3 studies the numerical simulation results of the proposed controllers. Finally, the conclusions are given in Section 4.

1 Dynamic Modeling

A conceptual graph of a solar power satellite[2] in orbit is shown in Fig. 1. It consists of an ultra-large solar array, a microwave transmitting antenna, a reflector, and other subsystems such as supporting structures. The ultra-large solar array should face to the Sun to capture solar radiation and generate electricity. This paper focuses on the attitude control of an ultra-large solar array as an example. The main objective is to improve attitude control accuracy while reducing the influences of structural vibrations and measurement noise.

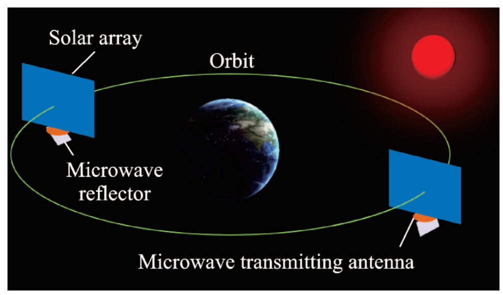

Fig.1 Conceptual graph of a solar power satellite in orbit

The flexible solar power satellite is simplified as a flexible Euler-Bernoulli beam moving in space (Fig.2). An inertial coordinate system OXY is constructed. Point A and Point B are two endpoints of the beam. The attitude control of the flexible beam is performed using two control moment gyros at Point A and Point B[19]. The control moments are denoted as M_A and M_B. The attitude control objec-

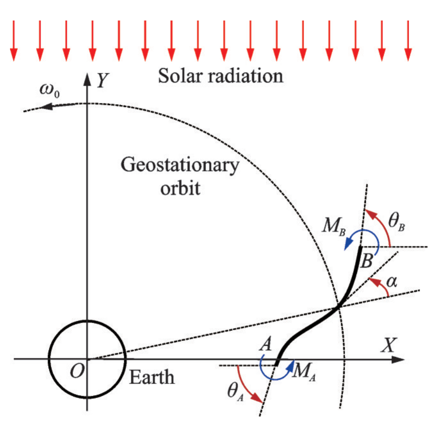

Fig.2 Orbit-attitude-structure coupled beam model

tive is that the beam remains parallel to OX axis under the influence of gravity gradient torque. The attitude errors are represented by θ_A and θ_B. The parameters of the flexible beam model are summarized in Table 1.

Table 1 Parameters of the simplified beam model

Parameter	Value
Length L/ m	1 200
Cross-sectional area A/ m^2	0.400 37
Second moment of area I/ m^4	0.001 591 2
Young's modulus E/ GPa	230
Density ρ/ (kg·m^{-3})	1 790
Number of element n	4
Degree of freedom	20

The beam is modeled by absolute nodal coordinate formulation considering the gravitational force and gravity gradient. The absolute nodal coordinate formulation is a well-known rigid-flexible coupled modeling method considering geometric nonlinearity. In this paper, a two-node Euler-Bernoulli beam element is adopted[20], and a two-dimensional dynamic model is established to reduce simulation time while it is able to simulate the orbit-attitude-structure coupled effects. The dynamic equations of the flexible beam can be written as[21]

$$\begin{cases} \dot{\boldsymbol{q}} = \boldsymbol{M}^{-1}\boldsymbol{p} \\ \dot{\boldsymbol{p}} = \boldsymbol{f}_{\text{ela}} + \boldsymbol{f}_{\text{gra}} + \boldsymbol{f}_{\text{con}} \end{cases} \tag{1}$$

where $\boldsymbol{q}$ is the generalized coordinate vector, $\boldsymbol{p}$ the termed generalized momentum vector, $\boldsymbol{M}$ the mass matrix, and $\boldsymbol{f}_{\text{ela}}$, $\boldsymbol{f}_{\text{gra}}$, $\boldsymbol{f}_{\text{con}}$ are the vectors of elastic force, gravitational force (including gravity gradient), and control force, respectively. The definition of nodal coordinates as well as the formulas of mass matrix and elastic force can be found in Ref.[20]. The formulation of the gravitational force was given in Ref.[22]. The control force vector $\boldsymbol{f}_{\text{con}}$ can be obtained by the principle of virtual work. The detailed modeling procedure is not given for simplicity.

The dynamic model in Eq.(1) is an orbit-attitude-structure coupled model. However, the orbital elements, such as the semi-major axis and eccentricity, are not changed in the simulations because the orbital perturbations are not considered. Thus, the orbital results are not given in the following simulations. The attitude motions of the beam (θ_A and θ_B) can be calculated from the generalized coordinate vector $\boldsymbol{q}$. In the simulations, the attitude motions are coupled with structural vibrations. The attitude disturbance considered in this paper is the gravity gradient torque. However, it is not easy to give the expression of the gravity gradient torque because it is influenced by the structural vibrations. For small deformation cases, the gravity gradient torque can be roughly estimated by

$$T = -\frac{3}{2} J\omega_0^2 \sin(2\alpha) \tag{2}$$

where $J = (mL^2)/12$ is the moment of inertia of the beam, ω_0 the orbital angular velocity, and α the attitude angle of the midpoint of the beam shown in Fig.2.

In the following numerical simulations, the beam moves in geostationary orbit ($\omega_0 = 7.292\,123 \times 10^{-5}$ rad/s). The beam is initially undeformed, located at the positive OX axis. The initial attitude errors are $\theta_A = \theta_B = 0$ and $\dot{\theta}_A = \dot{\theta}_B = 0$. In an ideal case, the attitude angle α would decrease linearly $\alpha = \alpha_0 - \omega_0 t$, and $\alpha_0 = 0$ is adopted in simulations.

Based on the above parameters, the maximum control moment is 823.2 N·m, and the required angular momentum storage is 1.13×10^7 N·m·s. In Ref.[7], a concept of space-assembled momentum wheel is proposed with a peak angular momentum of 4×10^8 N·m·s and a mass of 6 061 kg, which can be used in the attitude control of the solar array. Alternatively, 24 large control moment gyros can be adopted (250 kg and 500 000 N·m·s for each one)[7].

2 Control System Description

This section presents the implementation of the proposed self-tuning fuzzy ILC method. The attitude control objective is $\theta_A = \theta_B = 0$ such that the beam AB faces to the Sun. In practice, the attitude angles θ_A and θ_B should be measured by attitude sensors (such as Star trackers and Sun sensors) and then estimated using attitude filtering methods (such as extended Kalman filter approach). However, the attitude angles θ_A and θ_B are simply calculated from the generalized coordinate vector $\boldsymbol{q}$ in numerical simulations because attitude estimation is not the focus of this paper.

2.1 PD control

The control moments of the classic PD control law are calculated by

$$M_A = -k_p\theta_A - k_d\dot{\theta}_A \tag{3}$$

$$M_B = -k_p\theta_B - k_d\dot{\theta}_B \tag{4}$$

where k_d and k_p are the proportional and derivative feedback gains. The feedback gains are designed by

$$\begin{cases} k_d = 2\xi\omega_c J \\ k_p = \omega_c^2 J \end{cases} \tag{5}$$

where ω_c is the designed control frequency, and $\xi = 0.7$ the designed damping ratio of the controller. Although the PD control is a model-free control method, the control frequency should be selected manually. For a more complicated system such as the Multi-Rotary Joint Solar Power Satellite, the control frequencies for 50 solar arrays must be selected independently because of the different stiffness of the trusses[16].

2.2 Fuzzy PD control

In this subsection, a self-tuning fuzzy PD control method is studied for the flexible beam, based on the Mamdani fuzzy system. The objective of the fuzzy system is to select a minimum control frequency while meeting the control accuracy requirement. The fuzzy system is applied to M_A and M_B independently. The design process of the fuzzy controller includes fuzzification, rule-based inference, and defuzzification. For details of fuzzy control, please refer to Ref.[23].

Firstly, the function of the fuzzy system is to change the control gains according to the control error. In many fuzzy controllers, the fuzzy system works continuously using the real-time control error, which leads to frequent change of the control gains. To avoid this problem, the fuzzy system works once every half orbital period in the proposed fuzzy PD controller, because the period of the gravity gradient torque is half an orbital period as shown in Eq.(2). In other words, the control gains are adjusted every half orbital period according to the averaged control error. Therefore, the input of the fuzzy system is

$$e = \lg(\theta_a/\theta_r) \tag{6}$$

where θ_a is the average absolute value of the attitude error within half an orbital period, and θ_r a reference value of θ_a. The attitude control accuracy requirement is 0.5°, and the control error is usually a trigonometric function of time because the gravity gradient torque is also a trigonometric function of time, as shown in Eq.(2). Then, θ_a should be less than 0.32°, and the value of θ_r is selected as 0.32°. The difference between θ_a and θ_r is always within two orders of magnitude. Thus, the input domain can be taken as [−2,2].

The control frequency is adjusted by

$$\omega_{c2} = 10^k\omega_{c1} \tag{7}$$

where ω_{c1} and ω_{c2} are the control frequencies before and after the action of the fuzzy system, and k is the adjustment parameter (also the output of the fuzzy system). The value of k determines the variation speed of the control frequency. The domain of k in this paper is [−0.5, 0.5]. The use of logarithmic and exponential scale in Eqs.(6) and (7) enables the fuzzy system to handle a wide range of input and output.

Triangular membership functions for both input and output variables are employed, as shown in Fig.3 and Fig.4. In the membership distribution,

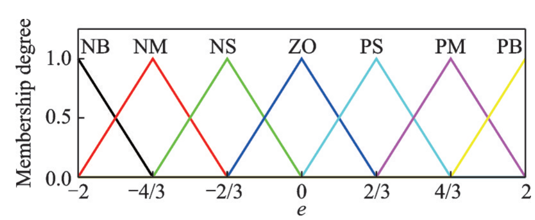

Fig.3 Membership function of input

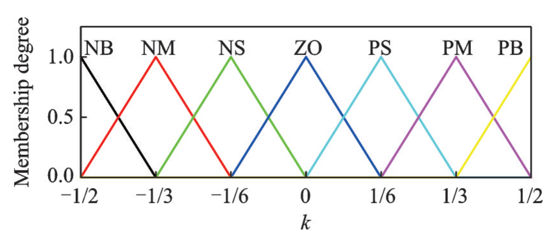

Fig.4 Membership function of output

the fuzzy variables are labeled with "N" "ZO" and "P" to represent "negative" "zero" and "positive", respectively. And the labels "B" "M" and "S" mean "big" "medium" and "small", respectively.

The rule-base inference is the key step for the fuzzy system design. According to the experience of attitude control of a flexible beam considering gravity gradient, the control errors decrease monotonously with the control frequency. When θ_a is larger than θ_r, ω_c needs to be increased. Therefore, a simple fuzzy rule can be established, as shown in Table 2. A rule in Table 2 can be interpreted as "If the input is NB, then the output is NB". The fuzzy system can adopt multiple inputs and multiple outputs according to practical requirements. The centroid formula is employed for defuzzification[23]. Combined with the input and output domains, a rule in Table 2 is interpreted as "If $\theta_a = 100\theta_r$, then $\omega_{c2} = \sqrt{10}\,\omega_{c1}$". The input domain should cover the concerned range of the attitude error. Then, the output domain should be determined by the desired variation speed of the control frequency.

Table 2 Fuzzy rule

Input	NB	NM	NS	ZO	PS	PM	PB
Output	NB	NM	NS	ZO	PS	PM	PB

In the implementation of the fuzzy PD control, the direct change of ω_c by Eq.(7) will lead to drastic changes in control moments. Therefore, a trigonometric function is adopted to change the control frequency smoothly. The transition time is 0.25 orbital periods, which is a half of the working period of the fuzzy system. The transition function is

$$\omega_c = \begin{cases} \omega_{c1} & t < \frac{i}{2}T \\ \frac{\omega_{c1}+\omega_{c2}}{2} - \frac{\omega_{c1}-\omega_{c2}}{2}\sin\left[\frac{4\pi}{T}\left(t-\frac{i}{2}T+\frac{1}{8}T\right)\right] & \frac{i}{2}T < t < \left(\frac{i}{2}+\frac{1}{4}\right)T \\ \omega_{c2} & t > \left(\frac{i}{2}+\frac{1}{4}\right)T \end{cases} \tag{8}$$

where $T = 86\ 164$ s is an orbital period and i denotes the ith orbital period.

2.3 Fuzzy ILC

Although the fuzzy PD control is able to adjust the control frequency according to the control error, it is a pure PD controller when the control frequency is converged to a certain value. The main problem of the PD controller is that the control moments are proportional to the control errors and the derivatives. The control errors can be reduced only if the control gains are increased. However, the influences of measurement noise are also increased.

In this section, a fuzzy ILC controller is proposed to improve the control accuracy by not increasing the control gains. The control moment of the ILC with a smooth switching parameter is calculated by[16]

$$M(t) = K_{FF}\overline{M}(t-T) + \boldsymbol{\Gamma}\boldsymbol{\theta}(t) \tag{9}$$

where K_{FF} is a switching parameter, $\boldsymbol{\Gamma} = [k_p, k_d]$ the matrix of feedback gains and $\boldsymbol{\theta} = [\theta, \dot{\theta}]^T$ the vector of control errors. For the first three periods, $K_{FF} = 0$ and the controller is a fuzzy PD controller. At the end of the 3rd period, the controller gradually becomes an ILC controller that use the control moments of the last period as feedforward control moments. Thus, the switching parameter is designed as[16]

$$K_{FF}(t) = \begin{cases} 0 & t < 3T \\ \frac{1}{2} - \frac{1}{2}\cos\left(\pi\frac{t-3T}{T}\right) & 3T < t < 4T \\ 1 & t > 4T \end{cases} \tag{10}$$

The reason to use fuzzy PD controller in the first three periods is that the control moments of the "previous" period are unavailable for the first period. Moreover, the fuzzy PD controller can reduce the initial attitude errors and provide more accurate feedforward control moments by adjusting the control frequencies in the first three periods.

It can be seen in Eq.(9) that the control moments of the last period is used directly to the current period if $\overline{M}(t-T) = M(t-T)$. However, the control moments of the last period contains other useless signals such as measurement noise and structural vibrations. Thus, the Fourier series is adopted to filter out useless historical signals based on the knowledge of gravity gradient torque, and $\overline{M}(t)$

is calculated by[16]

$$\overline{M}(t)=\frac{a_0}{2}+\sum_{n=1}^{N}\left(a_n\cos\frac{2n\pi t}{T}+b_n\sin\frac{2n\pi t}{T}\right) \tag{11}$$

where

$$a_n=\frac{2}{T}\int_0^T M(t)\cos\frac{2n\pi t}{T}\mathrm{d}t \tag{12}$$

$$b_n=\frac{2}{T}\int_0^T M(t)\sin\frac{2n\pi t}{T}\mathrm{d}t \tag{13}$$

The value of N can be selected according to the complexity of the attitude disturbance. In this paper, $N=10$ is selected because the gravity gradient torque in Eq.(2) is a simple sinusoidal function of time. The control gains are calculated by Eq.(5), and the control frequency is also adjusted by a fuzzy system. Thus, Eq.(9) is a fuzzy ILC controller.

When the controller is switched form fuzzy PD control to fuzzy ILC, the control errors would decrease significantly. The input domain of the fuzzy system can be expanded to $[-3,3]$ to avoid the input overflow of the fuzzy system, because the actual attitude errors might become three orders of magnitude smaller than the reference value. Other parameters of the fuzzy system are unchanged. In addition, since the control accuracy of ILC is much higher than the prescribed error θ_r, the fuzzy system tends to reduce ω_c to the maximum extent. However, the attitude of the flexible beam is unstable when ω_c is too small. Therefore, ω_c should not be less than an allowed minimum control frequency 1×10^{-4} in the simulation program by

$$\omega_c=\max(\omega_c,1\times10^{-4}) \tag{14}$$

Alternatively, the allowed minimum control frequency can be selected by another fuzzy system, which could be studied in future works.

3 Simulation Results

Measurement noise is considered in the following simulations. Gaussian white noise is used in the simulation program with an overall amplitude of 4×10^{-4} rad for attitude angle and 3×10^{-6} rad/s for angular velocity.

3.1 PD control

Firstly, the control results of the PD controller are studied for different control frequency ω_c, which varies from 5×10^{-5} to 5×10^{-3}. Simulation results are shown in Figs.5—7. It can be seen that due to the influence of periodic gravity gradient torque, the Sun-facing attitude errors and control moments of the PD controller also vary periodically. The maximum gravity gradient torque calculated using Eq.(2) is 823.2 N·m. The variations of the control moments in Fig.6 shows good agreement with theoretical results in Eq.(2), as the gravity gradient torque is counteracted by M_A+M_B. Whereas, the maximum value of M_A+M_B is 1 322 N·m, which indicates that measure noise has great influences on attitude control moments. With the increase of ω_c, the maximum errors θ_{max} decreases significantly. Thus, the control accuracy of the PD controller can be increased by increasing the feedback control gains. However, larger control gains also lead to more serious influences of measure noise on control moments.

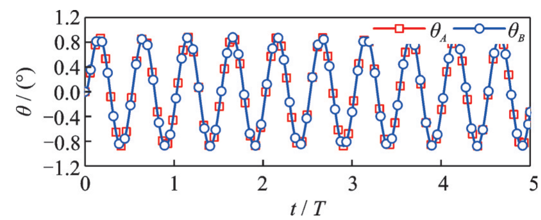

Fig.5 Errors of the PD control ($\omega_c=5\times10^{-4}$)

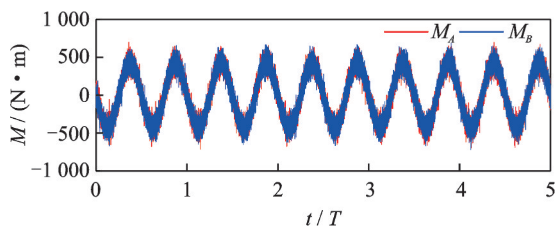

Fig.6 Moments of the PD control ($\omega_c=5\times10^{-4}$)

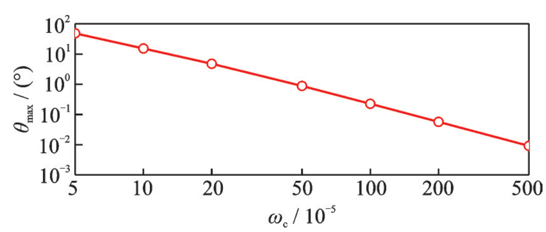

Fig.7 Maximum control errors for different control frequencies

3.2 Fuzzy PD control

A numerical simulation is conducted with an initial control frequency of $\omega_{c0}=5\times10^{-5}$ using the fuzzy PD controller. Simulation results are shown in Figs.8—10. At the beginning of the simulation, the control errors increase greatly because of the low control frequency. Then, the control frequency is increased by the fuzzy system, and finally converges to a value that the maximum control errors are approximately 0.5°. It can be seen in Fig.10 that the control frequency is adjusted every half orbital period by the fuzzy system. Moreover, the control frequency is changed smoothly during 0.25 orbital period. The influences of measurement noise are also increased as the control gains increase.

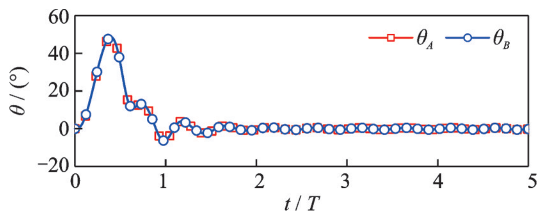

Fig.8 Errors of the fuzzy PD control ($\omega_{c0}=5\times10^{-5}$)

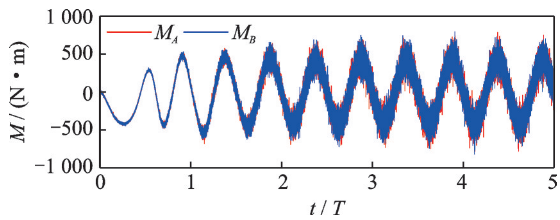

Fig.9 Moments of the fuzzy PD control ($\omega_{c0}=5\times10^{-5}$)

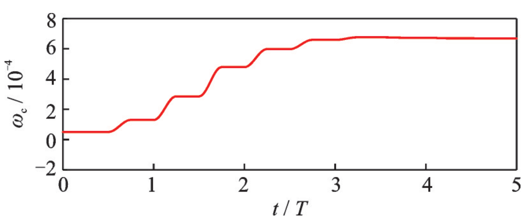

Fig.10 Control frequency of the fuzzy PD control ($\omega_{c0}=5\times10^{-5}$)

Another numerical simulation is carried out using a larger initial control frequency $\omega_{c0}=2\times10^{-3}$, as shown in Figs.11—13. At the beginning of the simulation, the control errors are small and the control moments are large. The measurement noise affects the control moments seriously. As the fuzzy system works, the control frequency and control moments are reduced gradually, while the control errors meet the control accuracy requirement. The control frequency converges to almost the same value as Fig.10. Thus, the fuzzy PD controller is able to achieve the required attitude control accuracy and adjust the control gain approximately.

However, the measurement noise has great influences on the control moments. The maximum values of M_A+M_B of the last period in Fig.9 and Fig.12 are over 1 360 N·m, which are much larger than the maximum value of gravity gradient torque (823.2 N·m). The reason is that the control accuracy and the influence of measurement noise are both proportional to the feedback gains, because the fuzzy PD controller becomes a pure PD controller when the control frequency is converged. Thus, the fuzzy ILC is proposed to improve control accuracy without increasing the feedback gains.

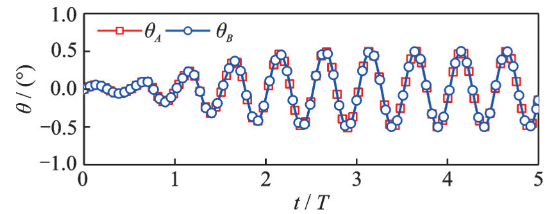

Fig.11 Errors of the fuzzy PD control ($\omega_{c0}=2\times10^{-3}$)

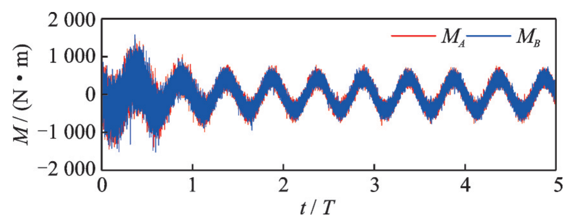

Fig.12 Moments of the fuzzy PD control ($\omega_{c0}=2\times10^{-3}$)

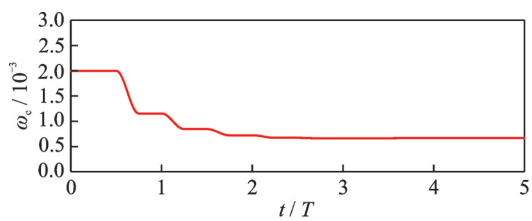

Fig.13 Control frequency of the fuzzy PD control ($\omega_{c0}=2\times10^{-3}$)

3.3 Fuzzy ILC

The fuzzy ILC is adopted in the numerical simulation, and the initial control frequency is $\omega_{c0}=5\times10^{-5}$. Simulation results are depicted in Figs.14—16. In the first three periods, the controller is a fuzzy PD controller, and the results are the same as

Figs.8—10. Whereas, when the fuzzy ILC is gradually switched on after three periods, the control errors are further decreased by using the control moments of last period as feedforward control moments. Consequently, the control frequency can be reduced by the fuzzy system. Moreover, the influences of measurement noise on the control moments are greatly reduced after the 4th period. The control frequency ω_c becomes 1×10^{-4} after six periods to ensure the attitude stability of the system.

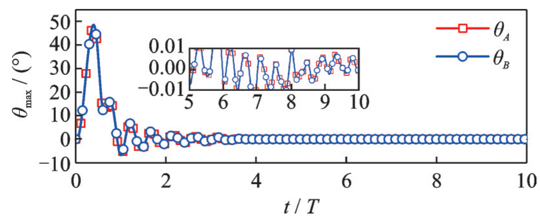

Fig.14 Errors of the fuzzy ILC ($\omega_{c0}=5\times 10^{-5}$)

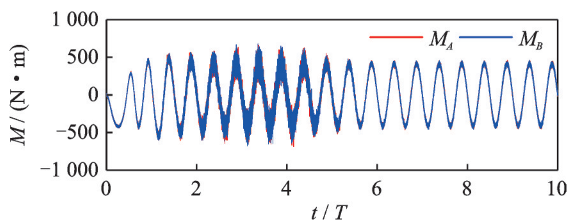

Fig.15 Moments of the fuzzy ILC ($\omega_{c0}=5\times 10^{-5}$)

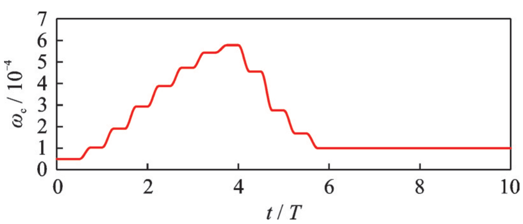

Fig.16 Control frequency of the fuzzy ILC ($\omega_{c0}=5\times 10^{-5}$)

The simulation with a large initial control frequency $\omega_{c0}=2\times 10^{-3}$ is also investigated, as shown in Figs.17—19. In the first three periods, the control frequency decreases under the effect of the fuzzy system because the control errors are very small. Thus, the control errors increase. As the controller is switched to the fuzzy ILC after three periods, the control errors, control frequency, and the influences of measurement noise are reduced significantly. The maximum values of M_A+M_B of the last period in Fig.15 and Fig.18 are less than 898 N·m. And the maximum attitude errors of the last period in Fig.14 and Fig.17 are less than 0.01°. Thus, the advantages of the proposed fuzzy ILC are small attitude control errors, small control moments, and self-tuning ability. The proposed controller can also be applied to the attitude control of large transmitting antenna in addition to the solar array, because the transmitting antenna requires 0.01° attitude accuracy.

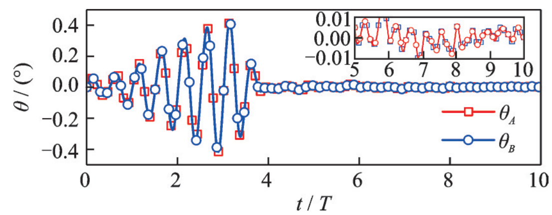

Fig.17 Errors of the fuzzy ILC ($\omega_{c0}=2\times 10^{-3}$)

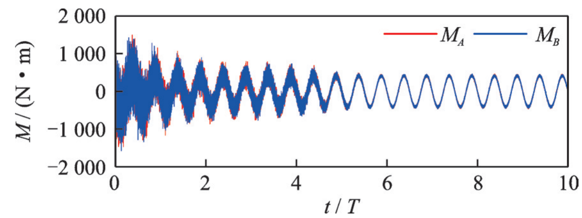

Fig.18 Moments of the fuzzy ILC ($\omega_{c0}=2\times 10^{-3}$)

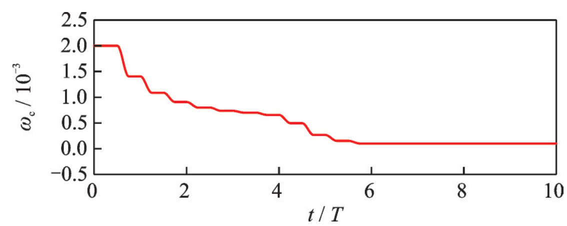

Fig.19 Control frequency of the fuzzy ILC ($\omega_{c0}=2\times 10^{-3}$)

The structural vibrations of Point B of the beam using fuzzy ILC with $\omega_{c0}=2\times 10^{-3}$ are shown in Fig.20. The structural vibration of Point B is estimated using a local coordinate system fixed at Point A. Structural vibrations are induced by the distributed gravity gradient and control moments. It can be seen that the structural vibration amplitude d is less than 0.4 m, which is very small compared to

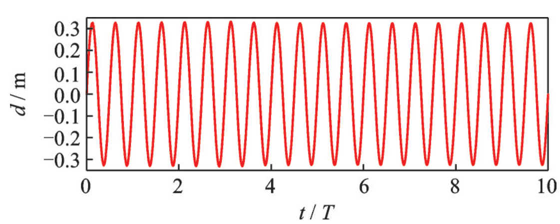

Fig.20 Structural vibration of Point B using fuzzy ILC ($\omega_{c0}=2\times 10^{-3}$)

the length of the beam.

3.4 Influences of structural vibrations

This subsection studies the validity of the proposed self-tuning fuzzy ILC for different system parameters. Particularly, when the Young's modulus is very small, the beam is extreme flexible and the gravity gradient could induce large-amplitude structural vibrations. Then the structural vibrations could greatly affect the attitude control accuracy. Thus, the Young's modulus is selected as $E=0.23$ GPa and $E=2.3$ GPa in the simulations, other parameters are not changed. The attitude controller is fuzzy ILC with initial control frequency of $\omega_{c0}=2\times10^{-3}$. Numerical results are depicted in Figs.21—24.

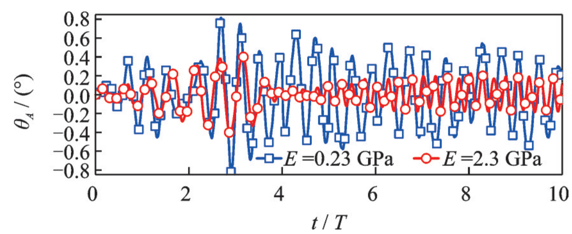

Fig.21 Errors of the fuzzy ILC with small Young's modulus ($\omega_{c0}=2\times10^{-3}$)

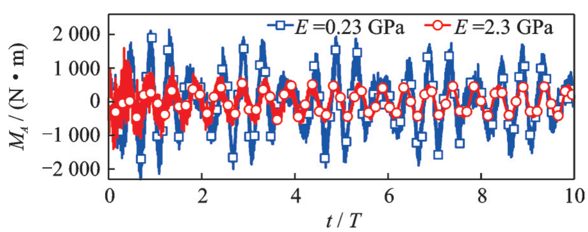

Fig.22 Moments of the fuzzy ILC with small Young's modulus ($\omega_{c0}=2\times10^{-3}$)

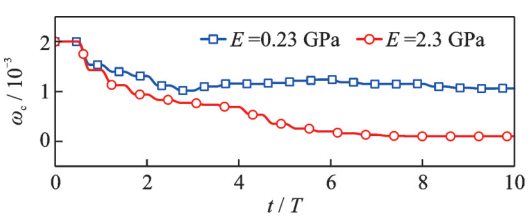

Fig.23 Control frequency of the fuzzy ILC with small Young's modulus ($\omega_{c0}=2\times10^{-3}$)

It can be found that the control errors of Point A are much larger than the above cases for $E=230$ GPa in Fig.14 and Fig.17. However, the maximum attitude errors in the last orbital period are

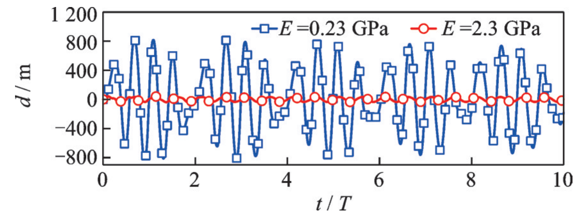

Fig.24 Structural vibration of Point B using fuzzy ILC with small Young's modulus ($\omega_{c0}=2\times10^{-3}$)

0.56° for $E=0.23$ GPa and 0.20° for $E=2.3$ GPa. The attitude error is just slightly larger than the required control accuracy for the extremely flexible beam. This problem can be solved by increasing θ_r slightly and performing structural vibration control of the beam[24]. In terms of control moments, the control moments for $E=0.23$ GPa is greatly influenced by structural vibrations. The maximum values of M_A+M_B in the last period are 2 713 N·m for $E=0.23$ GPa and 978 N·m for $E=2.3$ GPa. Moreover, the influences of measurement noise on the control moments are reduced dramatically for $E=2.3$ GPa. The control frequency for $E=0.23$ GPa is much larger than other cases, and it is not converged to a certain value at the end of the simulation. In contrast, the control frequency for $E=2.3$ GPa becomes 1×10^{-4} after eight orbital periods. It can be seen in Fig.24 that the maximum structural deformations are 825 m for $E=0.23$ GPa and 41.6 m for $E=2.3$ GPa. In summary, the proposed fuzzy ILC is validated to obtain the prescribed attitude control accuracy even if the beam is extremely flexible.

4 Conclusions

A self-tuning iterative learning control method is proposed for the attitude control of a flexible solar power satellite. The control frequencies of the PD control and ILC methods are adjusted automatically based on fuzzy logic. Although some parameters have to be selected for the proposed controller, such as the input/output domains and the transition time of the control frequency, they only affect the adjusting process of the control frequency, instead of the adjusting result. Thus, they are not required precisely. The main conclusions of this paper are as follows.

(1) The control frequency of the fuzzy PD controller is adjusted to a suitable value that the control errors are not larger than the prescribed error.

(2) The control errors are reduced greatly when the controller is switched from fuzzy PD control to fuzzy ILC.

(3) The influences of measurement noise are reduced as the decrease of the control frequency of the fuzzy ILC.

(4) The adjustment process is smooth by using the trigonometric function when changing the control frequency, so that the sudden changes of control moments are avoided.

References

[1] MANKINS J. A fresh look at space solar power: New architectures, concepts and technologies[J]. Acta Astronautica, 1997, 41(4/5/6/7/8/9/10): 347-359.

[2] MANKINS J, HOWELL J, O'NEIL D. New concepts and technologies from NASA's space solar power exploratory research and technology program[M]// Laying the Foundation for Space Solar Power: An Assessment of NASA's Space Solar Power Investment Strategy. USA: National Research Council of the National Academy of Sciences, 2001: 78-81.

[3] LIU Yuliang, WU Shunan, RADICE G, et al. Gravity-gradient effects on flexible solar power satellites[J]. Journal of Guidance Control and Dynamics, 2018, 41 (3): 773-778.

[4] LIU Jiafu, CUI Naigang, SHEN Fan, et al. Dynamic modeling and analysis of a flexible sailcraft[J]. Advances in Space Research, 2015, 56: 693-713.

[5] FIRUZI S, GONG Shengping. Attitude control of a flexible solar sail in low earth orbit[J]. Journal of Guidance, Control, and Dynamics, 2018, 41(8): 1715-1730.

[6] MENG Deshan, LU Weining, XU Wenfu, et al. Vibration suppression control of free-floating space robots with flexible appendages for autonomous target capturing[J]. Acta Astronautica, 2018, 151: 904-918.

[7] WIE B, ROITHMAYR C. Attitude and orbit control of a very large geostationary solar power satellite[J]. Journal of Guidance, Gontrol, and Dynamics, 2005, 28(3): 439-451.

[8] WU Shunan, ZHANG Kaiming, PENG Haijun, et al. Robust optimal sun-pointing control of a large solar power satellite[J]. Acta Astronautica, 2016, 127: 226-234.

[9] ZHANG Kaiming, WU Shunan, WU Zhigang. Multibody dynamics and robust attitude control of a MW-level solar power satellite[J]. Aerospace Science and Technology, 2021, 111: 106575.

[10] ARIMOTO S, KAWAMURA S, MIYAZAKI F. Bettering operation of robots by learning[J]. Journal of Robotic Systems, 1984, 1(2): 123-140.

[11] MOORE K, DAHLEH M, BHATTACHARYYA S. Iterative learning control: A survey and new results[J]. Journal of Robotic Systems, 1992, 9(5): 563-594.

[12] AHN H S, CHEN Yangquan, MOORE K. Iterative learning control: Brief survey and categorization[J]. IEEE Transactions on Systems, Man and Cybernetics Part C: Applications and Reviews, 2007, 37(6): 1099-1121.

[13] WANG Youqing, GAO Furong, DOYLE F. Survey on iterative learning control, repetitive control, and run-to-run control[J]. Journal of Process Control, 2009, 19(10): 1589-1600.

[14] WU Baolin, WANG Danwei, POH E K. High precision satellite attitude tracking control via iterative learning control[J]. Journal of Guidance, Control, and Dynamics, 2014, 38(3): 528-534.

[15] LI Qingjun, DENG Zichen, ZHANG Kai, et al. Precise attitude control of multirotary-joint solar-power satellite[J]. Journal of Guidance, Control, and Dynamics, 2018, 41(6): 1435-1442.

[16] LI Qingjun, WEI Yi, DENG Zichen, et al. Switched iterative learning attitude and structural control for solar power satellites[J]. Acta Astronautica, 2021, 182: 100-109.

[17] LI Jinsha, LI Junmin. Distributed adaptive fuzzy iterative learning control of coordination problems for higher order multi-agent systems[J]. International Journal of Systems Science, 2016, 47(10): 2318-2329.

[18] NOROUZI A, KOCH C. Robotic manipulator control using PD-type fuzzy iterative learning control[C]// Proceedings of 2019 IEEE Canadian Conference of Electrical and Computer Engineering (CCECE). [S. l.]: IEEE, 2019: 1-4.

[19] ZHANG Yong, MU Chaoxu, LU Ming. Data-based feedback relearning algorithm for robust control of SGCMG gimbal servo system with multi-source disturbance[J]. Transactions of Nanjing University of Aeronautics & Astronautics, 2021, 38(2): 225-236.

[20] ESCALONA J, HUSSIEN H, SHABANA A. Application of the absolute nodal co-ordinate formulation

to multibody system dynamics[J]. Journal of Sound and Vibration, 1998, 214(5): 833-850.

[21] LI Qingjun, DENG Zichen. Coordinated orbit-attitude-vibration control of a sun-facing solar power satellite[J]. Journal of Guidance, Control, and Dynamics, 2019, 42(8): 1863-1869.

[22] LI Qingjun, DENG Zichen, ZHANG Kai, et al. Unified modeling method for large space structures using absolute nodal coordinate[J]. AIAA Journal, 2018, 56(10): 4146-4157.

[23] YADAV A K, GAUR P. Improved self-tuning fuzzy proportional-integral-derivative versus fuzzy-adaptive proportional-integral-derivative for speed control of nonlinear hybrid electric vehicles[J]. Journal of Computational and Nonlinear Dynamics, 2016, 11(6): 061013.

[24] YANG Shaoxuan, HU Yu, SONG Zhiguang. Theoretical and experimental studies of active vibration control for beams using pole placement method[J]. Transactions of Nanjing University of Aeronautics & Astronautics, 2022, 39(1): 36-46.

Acknowledgements This work was supported by the Guangdong Basic and Applied Basic Research Foundation (No.2019A1515110730), the Young Elite Scientists Sponsorship Program by China Association for Science and Technology (No.2021QNRC001), and the Fundamental Research Funds for the Central Universities of Sun Yat-sen University (No.22qntd0703).

Authors Mr. **GAO Yuan** received his B.S. degree from School of Aeronautics and Astronautics, Sun Yat-sen University in 2022. His main research interest is control of solar power satellites.

Dr. **LI Qingjun** received the B.S. and Ph.D. degrees in engineering from Northwestern Polytechnic University, Xi'an, China, in 2014 and 2019, respectively. From 2019 to present, he has been with School of Aeronautics and Astronautics, Sun Yat-sen University as an assistant professor (master tutor). His main research interests include dynamics and control of solar power satellites, large space structures, and multibody spacecraft.

Author contributions Mr. **GAO Yuan** designed the control system, conducted the simulation and analysis and wrote the manuscript. Dr. **WU Shunan** contributed to the discussion of the control system and background of the study. Dr. **LI Qingjun** complied the dynamics models, summarized the conclusion and wrote the manuscript. All authors commented on the manuscript draft and approved the submission.

Competing interests The authors declare no competing interests.

(Production Editor: ZHANG Huangqun)

基于自调节迭代学习控制的柔性空间太阳能电站姿态控制

高 远，邬树楠，李庆军

(中山大学航空航天学院, 深圳 518107, 中国)

摘要:提出了柔性空间太阳能电站姿态控制的自调节迭代学习控制方法。将空间太阳能电站简化为在轨运行的欧拉-伯努利梁,采用绝对节点坐标法建立了轨道-姿态-结构耦合动力学模型。采用2个控制力矩陀螺实现姿态控制。为了提高经典比例-微分控制方法的控制精度,提出了切换迭代学习控制方法,采用以往周期控制力矩作为当前周期的前馈控制力矩。尽管迭代学习控制方法是一种无模型控制方法,其控制参数必须手动选择,给多可调参数的复杂控制系统设计带来困难。因此,采用模糊逻辑提出了一种自调节方法,可根据一个控制周期内平均控制误差自动调节控制器的控制频率。仿真结果表明,本文提出的控制方法可极大地提高控制精度,减小传感器噪声的影响,而且控制频率可自动调整至合适的值。

关键词:迭代学习控制;姿态控制;空间太阳能电站;模糊控制